but, because of flexibility in the backbone of the molecule, likely equilibrates through at least four distinguishable conformations. Empirical energy calculations indicate that electrostatic interactions are a major determinant of conformation in this molecule. MD simulations constrained by NOE distance information suggest that functional groups essential for biological activity maintain essentially the same relative orientations over the time course of the calculations. Although the reasons for the extremely tight binding of phallicidin to actin are not revealed by our conformational studies of the peptide, there is nothing apparent in these results to indicate what would be gained by a significant conformational deformation of phallicidin upon binding to actin. Our results may, therefore, prove useful in mapping the features of the actin-binding site that are complimentary to the structure of this peptide.

Acknowledgment. This work was supported by the California Cancer Research Coordinating Committee and, in part, by NIH Grant GM25975. We are indebted to Professor T. C. Bruice for access to his Silicon Graphics system and to D. H. Gregory for his assistance with some of the calculations.

Registry No. Phallacidin, 26645-35-2.

Multiple-Quantum NMR in a Mixture of Liquid Crystals: Differential Coherence Development[†]

W. V. Gerasimowicz,*,[‡] A. N. Garroway, and J. B. Miller

Contribution from the Chemistry Division, Code 6122, Naval Research Laboratory, Washington, D.C. 20375-5000. *Received October 31, 1989*

Abstract: A 2:1 molar mixture of 4′-(cyanophenyl)-4-*n*-heptylbenzoate and 4′-(cyanophenyl)-4-*n*-butylbenzoate exhibits nematic liquid crystal behavior in the temperature range from 25 °C to 50 °C. The proton NMR spectra suggest that two regimes of dipolar interaction are present, i.e., those characteristic of nearly isolated proton spin pairs, presumably on the phenyl rings, and weakly coupled multispin clusters originating from the alkyl chain moieties comprising the remainder of the system. A solid-echo pulse sequence permits the observation and separation of these unique regions within the molecules on the basis of their differing relaxation properties. We have combined this solid echo selection technique with multiple-quantum NMR. Differential development of proton spin coherence can then be distinguished (in this case) for *different* segments of the *same* molecule. We find that over the course of the multiple-quantum preparation times, the phenyl proton spin pairs do not interact appreciably with the remaining protons of the molecule.

Introduction

Time-resolved multiple-quantum nuclear magnetic resonance spectrometry (MQ NMR) has been demonstrated to be an effective means for determining the spatial distribution of nuclei in materials which lack long-range order. Much of the work has been performed in the liquid state where the size of spin systems which have been investigated is relatively small.[1-11] The operator formalism for double quantum NMR transitions of dipolar-coupled spin pairs (prior to the advent of time-reversal pulse sequences) has been discussed.[12] The introduction of time-reversal pulse sequences has made the investigation of larger spin systems, including those in solids, feasible.[13-15] Proton MQ NMR has been applied to NMR and imaging in solids,[16-19] the study of hydrogen distribution in solids,[14,19] and in the determination of hexamethylbenzene distribution in Na-Y zeolite samples.[20]

Nematic liquid crystals have also been the subject of a number of MQ NMR investigations.[11,15,21,22] In the case of nematic liquid crystal samples, intermolecular proton dipolar couplings are averaged to zero, while intramolecular couplings remain significant.[23] The elimination of intermolecular dipolar coupling is attributed to the rapid translational diffusion which nematic liquid crystalline molecules undergo. Such liquid crystal samples have been treated as idealized cases of isolated spin clusters on the NMR time scale, i.e., the individual molecules behave as if they are solid clusters which are independent of one another.[11,15,21,22] Furthermore, the development of multiple-quantum coherence within such systems (or the correlation of the ^{1}H spins within the molecule) has been analyzed on the basis that the pattern and rate of growth of such correlations reflects the distribution of atoms within the system.

In this article we present an example of a mixture of 4′-(cya-

---

* Author to whom correspondence should be addressed.

[†] Presented in part at the 29th Experimental Nuclear Magnetic Resonance Spectroscopy Conference, Rochester, NY, April 1988.

[‡] Permanent address: United States Department of Agriculture, Agricultural Research Service, North Atlantic Area, Eastern Regional Research Center, 600 E. Mermaid Lane, Philadelphia, PA 19118.

(1) Bodenhausen, G. *Prog. NMR Spectrosc.* **1981**, *14*, 137.
(2) Piantini, U.; Sorenson, O. W.; Ernst, R. R. *J. Am. Chem. Soc.* **1982**, *104*, 6800.
(3) Bax, A.; Freeman, R.; Kempsell, S. P. *J. Am. Chem. Soc.* **1980**, *102*, 4849.
(4) Bax, A.; Freeman, R.; Kempsell, S. P. *J. Magn. Reson.* **1980**, *41*, 349.
(5) Bax, A.; Freeman, R.; Frenkiel, T. A. *J. Am. Chem. Soc.* **1981**, *103*, 2102.
(6) Bax, A.; Freeman, R.; Frenkiel, T. A.; Levitt, M. H. *J. Magn. Reson.* **1981**, *43*, 478.
(7) Braunschweiler, L.; Bodenhausen, G.; Ernst, R. R. *Mol. Phys.* **1983**, *48*, 535.
(8) Levitt, M. H.; Ernst, R. R. *Chem. Phys. Lett.* **1983**, *100*, 119.
(9) Warren, W. S.; Weitekamp, D. P.; Pines, A. *J. Chem. Phys.* **1980**, *73*, 2084.
(10) Warren, W. S.; Pines, A. *J. Chem. Phys.* **1981**, *74*, 2808.
(11) Sinton, S.; Zax, D. B.; Murdoch, J. B.; Pines, A. *Mol. Phys.* **1984**, *53*, 333.
(12) Vega, S.; Pines, A. *J. Chem. Phys.* **1977**, *66*, 5624.
(13) Yen, Y. S.; Pines, A. *J. Chem. Phys.* **1983**, *78*, 3579.
(14) Baum, J.; Munowitz, M.; Garroway, A. N.; Pines, A. *J. Chem. Phys.* **1985**, *83*, 2015.
(15) Shykind, D. N.; Baum, J.; Liu, S.-B.; Pines, A.; Garroway, A. N. *J. Magn. Reson.* **1988**, *76*, 149.
(16) Drobny, G.; Pines, A.; Sinton, S.; Weitekamp, D. P.; Wemmer, D. *Faraday Symp. Chem. Soc.* **1979**, *13*, 49.
(17) Bodenhausen, G.; Vold, R. L.; Vold, R. R. *J. Magn. Reson.* **1980**, *37*, 93.
(18) Pines, A. In *Proceedings of the Fermi School on the Physics of NMR in Biology and Medicine*; Maraviglia, B., Ed.; In press.
(19) Garroway, A. N.; Baum, J.; Munowitz, M. A.; Pines, A. *J. Magn. Reson.* **1984**, *60*, 337.
(20) Ryoo, R.; Liu, S.-B.; de Menorval, L. C.; Takegashi, K.; Chmelka, B.; Trecoske, M.; Pines, A. *J. Phys. Chem.* **1987**, *91*, 6575.
(21) Sinton, S.; Pines, A. *Chem. Phys. Lett.* **1980**, *76*, 263.
(22) Munowitz, M.; Pines, A. *Science* **1986**, *233*, 525.
(23) De Gennes, P. G. *The Physics of Liquid Crystals*; Clarendon Press: Oxford, 1974.

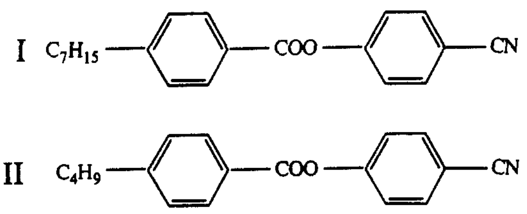

Figure 1. Nematic liquid crystal composition: 2:1 molar mixture of 4′-(cyanophanyl)-4-*n*-heptylbenzoate (I) and 4′-(cyanophanyl)-4-*n*-butylbenzoate (II).

nophenyl)-4-*n*-heptylbenzoate and 4′-(cyanophenyl)-4-*n*-butylbenzoate which exhibits nematic liquid crystal behavior.[24] The structures of these molecules are depicted in Figure 1. The development of dipolar interactions is more complex for this liquid crystal in that the proton spin coherence does not develop uniformly within the molecules themselves. Data are presented to illustrate such behavior, and an analysis of cluter size is shown based upon the separation of the distinct intramolecular dipolar interactions.

Multiple-Quantum Coherence and Dipolar Selection. Because nematic liquid crystals undergo rapid diffusion, the intermolecular dipolar couplings are negligible or insignificant. Even so, the conventional dipolar-coupled spectrum, obeying the selection rule $\Delta M = \pm 1$, from even a small number of oriented spins is rather featureless. Such single-quantum spectra in themselves do not provide enough information to determine the atomic distribution(s) of the proton nuclei. On the other hand, MQ NMR, by creating high-order multiple-quantum coherences, can simplify the spectra[16,17,25] and also, by multiple-quantum spin-counting methods, probe the nature, extent, and isolation of proton clusters in chemical and physical systems.[14,15,19] Thorough reviews on MQ NMR theory have been previously published.[1,26] Here we are primarily interested in identifying the size of the spin system where partially isolated protons are present, as reflected in the time dependence of the MQ intensities.

The eight-pulse sequence[15] shown in Figure 2 generates an average dipole Hamiltonian:

$$\langle \mathcal{H}_{\mathrm{D}} \rangle = \tfrac{1}{3}(\mathcal{H}_{yy} - \mathcal{H}_{xx}) \qquad (1)$$

where $\mathcal{H}_{zz}$ is the customary high-field homonuclear dipolar Hamiltonian quantized along the z direction. This Hamiltonian consists solely of double-quantum operators and so excites only even-order MQ coherences. For the present spin-counting purposes, we use the method of phase-incremented MQ NMR[15] in which the evolution period (t_1) is kept fixed, while the phase of the Hamiltonian in the preparation period τ is incremented relative to its phase during the mixing time (τ). The resulting MQ spectra are infinitely narrow in the t_1 frequency domain.

During the preparation period, the intensities of the MQ coherences are redistributed to higher order at the expense of lower order coherences. In order for spins to become correlated in this way, the Hamiltonian operator must act for a time which is at least comparable to the inverse of the proton dipolar interactions. As the coupling constant is inversely proportional to the cube of the interproton distance, nearby spins interact over short time frames, whereas spins which are farther apart require relatively more time to communicate. If a solid contains isolated clusters, the dipolar couplings among groups may be negligible, and an upper limit may be imposed on the number of interacting nuclei. By contrast, for a continuous distribution of spins, the effective system size would continually increase over (preparation) time. Therefore, a series of MQ experiments of varying preparation times can be used to determine the effective system size and whether nuclei are clustered or homogeneously distributed. To these well-known ideas, we add the following option. We start the spin system in one of two different initial states: (i) the conventional state in which all spins on the molecule have equilibrium polarization and (ii) a dipolar selected state in which only those spins which are in more or less isolated spin pairs have a nonzero population. Condition (ii) is easily approximated by use of a solid echo sequence prior to the MQ preparation period, as shown in Figure 2. A 90_x–τ_{dip}–90_y sequence creates a solid echo at time $2^*\tau_{\mathrm{dip}}$. For dipolar-coupled pairs of spin 1/2 nuclei, such a pulse sequence refocuses all the magnetization, independent of the pulse spacing and size of the coupling. In general, for more than two coupled spins, the magnetization is only partially refocussed, and the refocussing efficiency depends on the ratio of τ_{dip}/T_2. Hence this solid echo provides a convenient way to select out isolated, strongly coupled spin pairs by setting τ_{dip} much longer than the effective T_2 of the weakly coupled multispin system. We used a τ_{dip} of 200 μs. We shall find that the dipolar echo spin pairs remain essentially isolated from the rest of the molecule even over times which are long compared to T_2.

Experimental Section

Reagent grade 4′-(cyanophenyl)-4-*n*-heptylbenzoate and 4′-(cyanophenyl)-4-*n*-butylbenzoate were purchased from Aldrich Chemical Co. and utilized as received. (Reference to brand or firm name does not constitute endorsement by any agency of the United States Government over others of a similar nature not mentioned.) The nematic mixture was prepared in an exact 2:1 molar proportion and exhibits nematic liquid crystal behavior in the temperature range from 25 °C to 50 °C.[27] All spectroscopic measurements were made in the nematic liquid crystal temperature regime. Sample heating due to long rf pulse trains was not evident. All of the NMR spectra were acquired on a homebuilt multiple quantum spectrometer operating at a frequency of 100 MHz for the proton resonance. The proton single-quantum spectra were obtained by the standard Fourier transform method by using solid echo detection ($\tau_{\mathrm{dip}} = 5$ μs) to avoid receiver recovery delay. Phase-incremented multiple quantum spectra[15] were obtained with the pulse sequence shown in Figure 2. The experimental parameters employed were $\Delta = 2.0$ μs, $\Delta' = 8.0$ μs, fixed $t_1 = 2.0$ μs, $\tau_{90} = 4.0$ μs, and $1 \leq \tau/\tau_{\mathrm{C}} \leq 60$. The basic cycle time τ_{C} was 72 μs. For the optional solid echo selection 90_x–τ_{dip}–90_y, with $\tau_{\mathrm{dip}} = 200$ μs, a 90_{-x} pulse was applied at $2^*\tau_{\mathrm{dip}}$ to restore magnetization to the z direction; the MQ experiment was initiated after a 500-μs delay (Figure 2). Detection was by pulsed spin locking for 1 ms after the mixing period. The sequence was phase cycled to remove the undesirable (for our purposes) odd-order MQ coherences by cycling the pulse phases during the preparation period between 0° and 180° in alternate experiments and coadding the resulting signals.

Results and Discussion

Since the spatial arrangements of atoms are reflected by the magnitudes of their dipolar couplings, time-dependent multiple-quantum experiments yield results concerning the distribution of spins in a system. The calculation of the growth of the distribution of coherence in proton spin systems relates the intensity distribution of the signal over the MQ orders to the number of correlated spins at that particular instant. Previous workers have shown that the calculation of the growth of the distribution of coherence can be reduced to a combinatorial problem.[28-30] Such calculations make the simplifying assumption that all possible coherences can be excited with equal probability. For a spin system of N spin 1/2 particles, the number of transitions between coherent states differing by $n = \Delta M$ is just

$$\binom{2N}{N - \Delta M} = 2N!/(N - \Delta M)!(N + \Delta M)! \qquad (2)$$

In particular, an N-spin system will not support coherences above MQ order N. Equation 2 is well-approximated by a Gaussian distribution for $N > 6$. Therefore, the multiple-quantum intensity distribution, $I(n)$, may be described by a Gaussian curve

$$I(n) = \exp(-n^2/N) \qquad (3)$$

with a variance of

$$\sigma = (N/2)^{1/2} \qquad (4)$$

---

(24) Boller, A.; Scherrer, H.; Schadt, M. *Proceedings IEEE* **1972**, 1002.

(25) Aue, W. D.; Bartholdi, E.; Ernst, R. R. *J. Chem. Phys.* **1976**, *64*, 2229.

(26) Weitekamp, D. P. *Advances in Magnetic Resonance*; Waugh, J. S., Ed.; Academic Press: Vol. 11, pp 111–274.

(27) Boller, A.; Scherrer, H.; Schadt, M. *Proceedings IEEE* **1972**, 1002–1003.

(28) Hoffman, R. A. *Adv. Magn. Reson.* **1970**, *4*, 87.

(29) Wokaun, A.; Ernst, R. R. *Mol. Phys.* **1978**, *36*, 317.

(30) Murdoch, J. B.; Warren, W. S.; Weitekamp, D. P.; Pines, A. *J. Magn. Reson.* **1984**, *60*, 205.

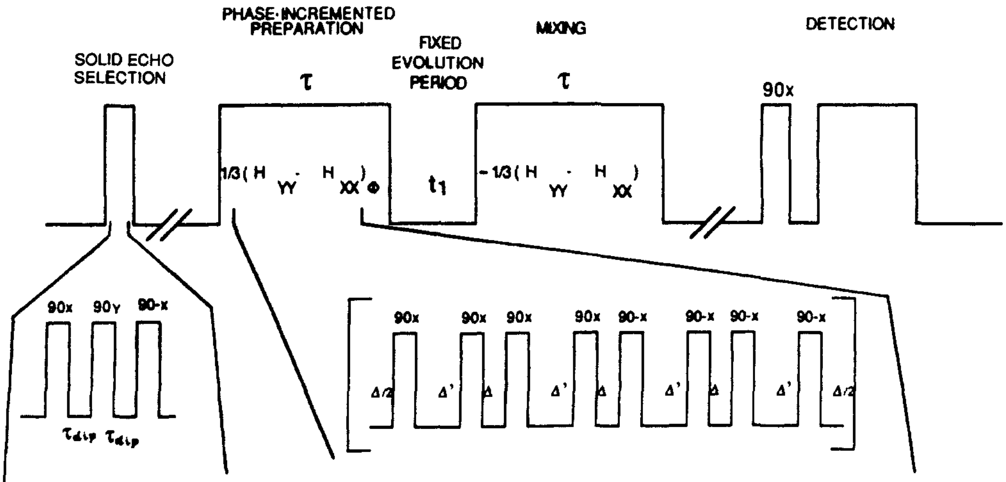

Figure 2. MQ NMR pulse sequence: Δ = 2.0 μs, Δ' = 8.0 μs, fixed t_1 = 2.0 μs, τ_{90} = 4.0 μs, and 1 ≤ τ/τ_C ≤ 60. The basic cycle time τ_C was 72 μs. For the optional solid echo selection 90_x–τ_{dip}–90_y, with τ_{dip} = 200 μs, a 90_{-x} pulse was applied at $2^*\tau_{dip}$ to restore magnetization to the z direction followed by the MQ experiment after a delay of 500 μs. Detection was by pulsed spin locking.

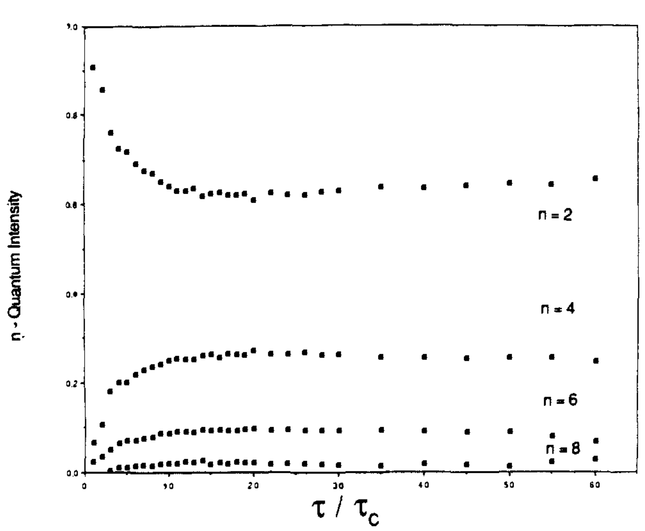

Figure 3. Normalized MQ intensities of the n = 2 to n = 8 peaks versus τ/τ_C for the nematic liquid crystal. The basic cycle time τ_C was 72 μs.

This highly simplified picture applies to the "equilibrium" distribution of MQ coherence within the spin system. It is expedient to regard the effective system size N as a time-dependent parameter, reflecting the effective number of spins among which dipolar coupling has been achieved during a given preparation period.[28-30] One then fits the integrated intensities of the MQ transitions to a Gaussian and associates the σ of the Gaussian with $(N(\tau)/2)^{1/2}$. Figure 3 shows a plot of the proton n-quantum intensity, without dipolar selection, for the 2:1 nematic liquid crystal examined in this work (normalized to the total intensity) vs τ/τ_C. At short preparation times, the number and intensities of the MQ orders are seen to increase. Beyond about τ/τ_C = 10, a plateau is reached. This behavior points to a constant value for the overall system size, i.e., the effective system size does not increase beyond some limit characteristic of the apparent cluster size. The composition of the nematic liquid cyrstal is such that a 2:1 ratio of 23 spins to 17 spins is present. Assuming for the moment that all the spins on each molecule participated in the MQ evolution, one would expect to see a superposition of two Gaussians, in a 2:1 intensity ratio, with respective spin sizes of 23 and 17 spins. As it is unlikely that these two Gaussians could be resolved, their superposition would appear as a single Gaussian with an apparent size of $[(1/3)(2^*23^2 + 17^2)]^{1/2}$ or an rms average of approximately 21 spins per "average" molecule comprising the mixture. For our MQ results without dipolar selection, all attempts (not shown) to approximate the overall cluster size by means of single binomial and/or Gaussian distributions met with failure in that the observed MQ intensities did not fit the calculations, and at best the method underestimated the numbers of protons expected in this case. Anomalous values of approximately 13–14 correlated spins were calculated at maximum preparation times utilizing this approach.

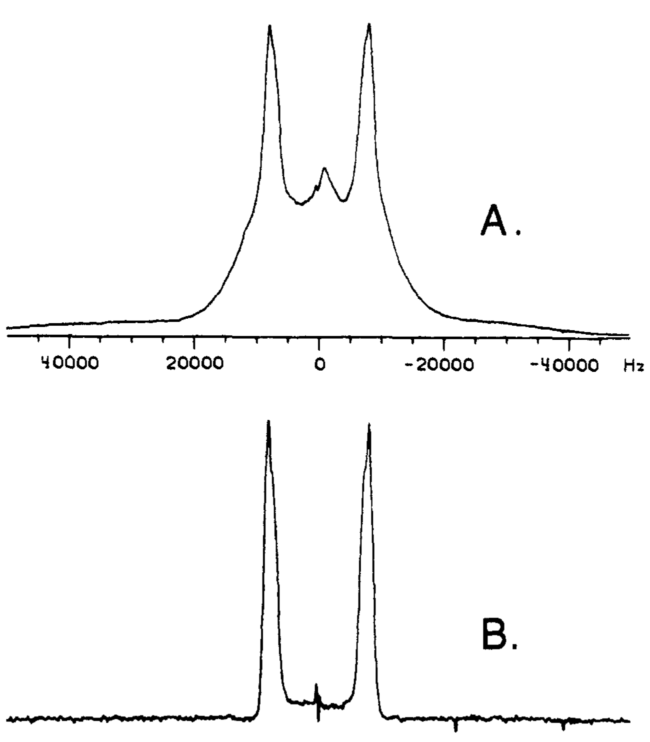

Figure 4. A. ^{1}H NMR spectrum of the nematic liquid crystal which was obtained with solid echo detection (τ_{dip} = 5 μs). With this short delay time, no change in the proton intensities for either of the two proton spin subsystems is observed. B. Solid echo selected ^{1}H NMR spectrum of the nematic liquid crystal. The pulse sequence employed for the solid echo selection was 90_x–τ_{dip1}–90_y–τ_{dip1}–90_{-x}–τ_d–90_x–τ_{dip2}–90_y–τ_{dip2}–acquisition. The first solid echo, with τ_{dip1} = 200 μs, separated the two different spin subsystems. The second solid echo, with τ_{dip2} = 5 μs, is used to avoid receiver recovery delay. The two solid echoes are separated by a delay, τ_d = 500 μs.

The origin of this apparent discrepancy between the average system size of 21 spins and the smaller apparent size is easily seen by examining the single-quantum spectrum in Figure 4A: the ^{1}H spectrum consists of a central peak and a doublet. The doublet splitting of approximately 15 kHz is consistent with the dipolar coupling exhibited by isolated proton pairs. Isolated proton pairs are evident on all of the rigid phenyl rings of the liquid crystal

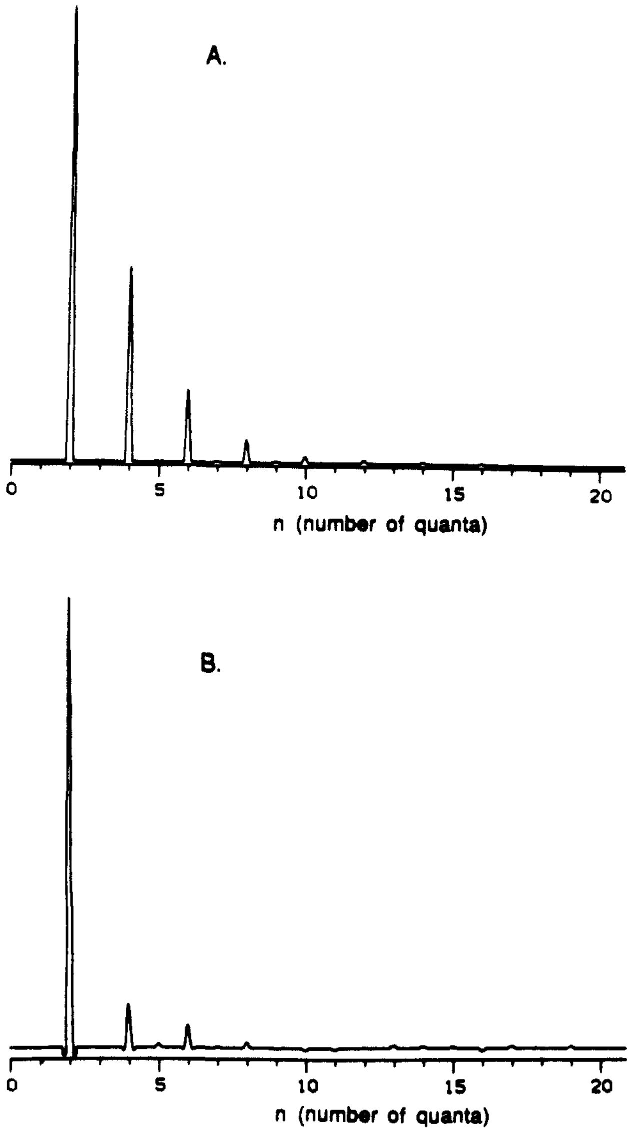

Figure 5. A. Phase-incremented multiple-quantum NMR spectra of the nematic liquid crystal (without solid echo selection) where $\tau/\tau_C = 16$ and the basic cycle time, $\tau_C = 72$ μs. B. Phase-incremented multiple-quantum NMR spectra of the nematic liquid crystal after solid echo selection of the two-spin subsystem. The conditions are the same as in part A with $\tau_{dip} = 200$ μs and a 500-μs delay between the solid echo selection and the start of the MQ excitation sequence.

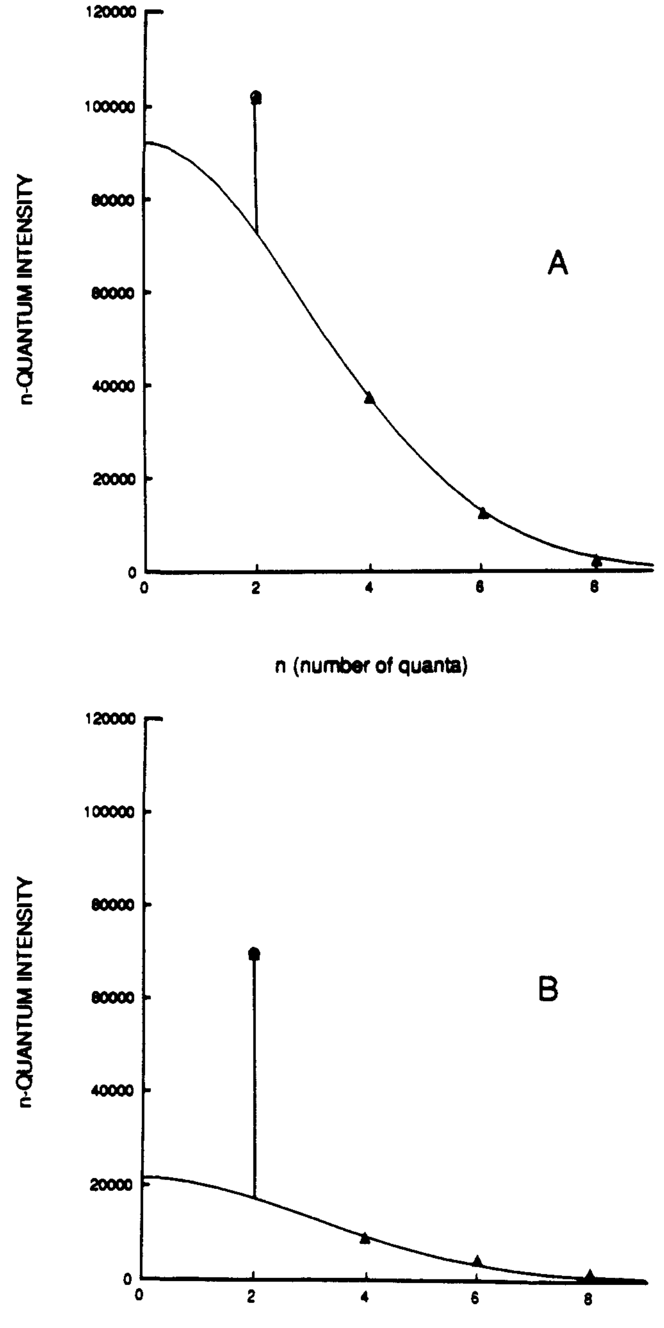

Figure 6. Curve fits and experimental MQ nematic liquid crystal data: $\tau/\tau_C = 16$; (▲) MQ experimental intensities; (○) fit of the MQ intensities to eqs 5a and 5b; solid lines represent Gaussian curve fits and superposition of the two-spin subsystem intensity. A. Fit of the phase-incremented multiple-quantum NMR data of Figure 5A. This data was obtained without solid echo selection. B. Fit of the phase-incremented multiple-quantum NMR data of Figure 5B. This data was obtained after solid echo selection of the two-spin subsystem.

molecules comprising the system examined in this paper. The splitting of approximately 15 KHz is consistent with that predicted by calculation of this effect for adjacent protons on a phenyl ring. The central peak arises from methyl and alkyl chain protons. These two proton populations have been distinguished previously in nematic liquid crystals by selective deuteration.[32] If the alkyl tails are deuterated in such systems, only a doublet from the two-spin portions of the phenyl groups is seen.

We can separate and observe these unique regions within the nematic liquid crystal in the conventional proton spectrum on the basis of their differing T_2 relaxation properties by application of a solid-echo pulse sequence[33] to produce the spectrum in Figure 4B. As discussed above, setting a long solid echo time preserves magnetization from the spin pairs while discriminating against multispin systems, even if rather weakly coupled. This discrimination is quite effective. Examination of the data in Figure 4B indicates that the relative contributions of the alkyl chain protons have been reduced to a negligible quantity compared to their intensities in Figure 4A. In Figure 5 we see the result of MQ coherence development for the case of the system using standard, nonselective (ns) MQ NMR, and for the case when a solid echo selective (ses) sequence has been inserted prior to the start of the MQ NMR sequence. The qualitative difference is striking. In Figure 5A one observes strong two-, four-, and six-order coherences with smaller higher order coherences out to about $n = 10$; in Figure 5B the predominant coherence in the solid echo selected MQ spectrum is only two-quantum, with much smaller four- and six-quantum lines visible: the proton pairs do not interact ap-

---

(31) Baum, J.; Pines, A. *J. Am. Chem. Soc.* **1986**, *108*, 7447.

(32) Charvolin, J.; Deloche, B. Nuclear Magnetic Resonance Studies of Molecular Behavior. In *The Molecular Physics of Liquid Crystals*; Luckhurst, G. R., Gray, G. W., Eds.; Academic Press: pp 343–366.

(33) Mansfield, P. Multiple-Pulse Nuclear Magnetic Resonance Transients in Solids. *Phys. Rev.* **1965**, *137*, A961–A974.

preciably with the remaining alkyl protons of the molecule. Thus, differential development of proton spin coherence can be distinguished (in this case) for *different* segments of the *same* molecule. The higher order ($n > 2$) coherences in Figure 5B do not grow much even for longer preparation times, and we regard their presence primarily as artifacts arising from imperfect discrimination between multispin clusters and nearly isolated spin pairs by the solid echo sequence, rather than a leakage of order to other parts of the molecule.

The observed MQ intensities, without solid echo selection, can now be analyzed since we have evidence that the overall spin system is a superposition of a small, primarily two-spin subsystem, with a larger, more weakly coupled system from the alkyl chain protons. We model the intensity of the n-order coherence in the (nonselective) MQ spectrum as a superposition of a Gaussian for the larger subsystem and a two spin system

$$I_{\mathrm{obs}_{\mathrm{ns}}}[n(\tau)] = M_{\mathrm{g}} \exp[-n(\tau)^2/N_{\mathrm{e}}] + M_2[\delta(0) + \delta(2)] \qquad (5a)$$

where $\delta(0)$ and $\delta(2)$ represent the intensities of the zero- and two-quantum coherences due to the two-spin subsystems, and N_{e} is the effective system size for the larger subsystem. There are also some normalization factors (M_{g} and M_2) to be accounted for. For the solid echo selected MQ sequence, we would expect M_{g} to be zero in eq 5, provided the solid echo selection worked perfectly. These contributions of the higher order coherences to the solid echo selected MQ spectrum are small though not zero, cf. Figure 5b, and the details of how they are handled do not affect the general conclusions. We allow a fraction (ϵ) of the Gaussian to persist:

$$I_{\mathrm{obs}_{\mathrm{ses}}}[n(\tau)] = c([\epsilon M_{\mathrm{g}} \exp[-n(\tau)^2/N_{\mathrm{e}}] + M_2[\delta(0) + \delta(2)]]) \qquad (5b)$$

Here c is a constant describing the efficiency of the solid echo sequence relative to eq 5a. Note that in these experiments the zero-order coherence is not recorded.

At each preparation time, analysis proceeds by fitting the $n > 2$ coherences of the nonselective MQ spectrum to the Gaussian in eq 5a, determining the two-spin contribution to the two-quantum coherence, and then extracting ϵ from eq 5b. ϵ is found to be more or less independent of the preparation time τ, indicating that the higher order coherences in the solid echo selected MQ spectrum are indeed due to the inefficiency of the solid echo selection and do not come predominantly from two spin systems. Experimental MQ data and a representative fit are shown in Figure 6.

The number of spins which are in the two-spin system can now be calculated: (i) the number of spins in the N spin system and its integrated intensity, I_{g}, (over all coherences) is known. The integrated intensity, I_2, of the two-spin system can also be calculated by noting that the zero- and two-quantum intensities are equal (eq 2) and then the number of protons in the two-spin systems is calculated as $N_2 = (I_2/I_{\mathrm{g}})^*N$.

We find that over a wide range of preparation times ($10 \leq \tau/\tau_{\mathrm{C}} \leq 60$), $N = 13 \pm 1$, and from the ratio of M_{g}/M_2 and appropriate normalizations for the Gaussian and two-spin systems, there are eight protons in two-spin systems for every 13-spin system. This result is consistent with the structure of the liquid crystal mixture: for the "average" molecule there are eight phenyl protons and 15 and 9 alkyl protons, in a 2:1 ratio, respectively. If these two respective Gaussians are not resolved, we should expect a single Gaussian with an effective size of 13.3 spins, quite close to our result of 13 ± 1.

Conclusions

The development of MQ coherence is the result of the concerted interaction of numerous spins in a solid. The development is dynamic and is first dominated by the largest couplings present. While all spins would in principle be affected by every spin present, we have presented a case where the distance separating spins can actually isolate collections or intramolecular clusters as seen in the data presented. Furthermore, the differential relaxation properties (in this case, T_2 and the special properties of two-spin dipolar couplings) of a molecule may be effectively utilized to focus upon and distinguish groups of nuclei within a molecule where their contributions to the overall development of MQ coherence are limited by their geometry, internal motions, or separation from other dipolar species. We have employed a highly simplified model to account for the gross features of the MQ development of the two subsystems, the alkyl chain protons, and sets of spin pairs on the phenyl head groups.

Solid-State Voltammetry and Self-Diffusion Dynamics of a Linear Monotagged Redox Polymer: ω-Ferrocenecarboxamido-α-methoxypoly(ethylene oxide)

M. J. Pinkerton, Y. Le Mest,[†] H. Zhang, M. Watanabe,[‡] and Royce W. Murray*

Contribution from the Kenan Laboratories of Chemistry, University of North Carolina, Chapel Hill, North Carolina 27599-3290. *Received November 6, 1989*

Abstract: The synthesized title labeled polymer, Fc-MePEG, MW = 2590, analytically characterized as free of unlabeled PEO and of ferrocene monomer, dissolves $LiClO_4$ electrolyte and in dry undiluted form is both a polymer electrolyte and an electroactive phase. The microelectrode solid-state voltammetrically measured, center-of-mass self-diffusion coefficient for Fc-MePEG in its polymer melt, 1.3×10^{-8} cm²/s at 62 °C, is 3.4 times smaller than that for ferrocene monomer dissolved in unlabeled (MW = 2380) Me_2PEG. Electron hopping is estimated to contribute less than 10% to the diffusion rates of Fc-MePEG and of monomer dissolved at 40–50 mM concentrations in unlabeled Me_2PEG. At room temperature, where Fc-MePEG and Me_2PEG are waxy solids, $D_{\mathrm{Fc\text{-}MePEG}}$ is 3.9×10^{-12} cm²/s, 12 times smaller than that of monomer ferrocene, in Me_2PEG, and which corresponds to a diffusion pathlength of ca. 110–200 nm during the electrochemical experiment. Dissolved in CH_3CN or CH_2Cl_2, Fc-MePEG diffuses 8–10 times more slowly than ferrocene monomer which is consistent with transport as a random coiled sphere.

This paper describes the voltammetric determination of the center-of-mass self-diffusion coefficient of a linear polymer chain bearing a single redox end group (ferrocene), in the pure polymer phase, and as a polymer solution in unlabeled polymer of similar MW. ω-Ferrocenecarboxamido-α-methoxypoly(ethylene oxide), $CpFeCpCONH(CH_2CH_2O)_nCH_3$ (Fc-MePEG), was synthesized[1]

[†] Current address: U.A. C.N.R.S. 322, Departement de Chimie, Universite de Bretagne Occidentale, 6 Avenue Le Gorgeu, 29287 Brest, Cedex, France.

[‡] Permanent address: Department of Chemistry, Sophia University, 7-1 Kioi-cho, Chiyoda-ku, Tokyo 102, Japan.

(1) Zalipsky, S.; Gilon, C.; Zilkha, A. *Eur. Polym. J.* **1983**, *19*, 1177.

0002-7863/90/1512-3730$02.50/0